Comparison of pause predictions of two sequence-dependent transcription models

J. Stat. Mech. (2010) P12007

(http://iopscience.iop.org/1742-5468/2010/12/P12007)

Journal of Statistical Mechanics: Theory and Experiment
An IOP and SISSA journal

Comparison of pause predictions of two sequence-dependent transcription models

Lu Bai[1] **and Michelle D Wang**

Department of Physics, Laboratory of Atomic and Solid State Physics, Cornell University, Ithaca, NY 14853, USA
E-mail: lbai01@rockefeller.edu and mdw17@cornell.edu

Received 1 September 2010
Accepted 5 November 2010
Published 1 December 2010

Online at stacks.iop.org/JSTAT/2010/P12007
doi:10.1088/1742-5468/2010/12/P12007

Abstract. Two recent theoretical models, Bai *et al* (2004, 2007) and Tadigotla *et al* (2006), formulated thermodynamic explanations of sequence-dependent transcription pausing by RNA polymerase (RNAP). The two models differ in some basic assumptions and therefore make different yet overlapping predictions for pause locations, and different predictions on pause kinetics and mechanisms. Here we present a comprehensive comparison of the two models. We show that while they have comparable predictive power of pause locations at low NTP concentrations, the Bai *et al* model is more accurate than Tadigotla *et al* at higher NTP concentrations. The pausing kinetics predicted by Bai *et al* is also consistent with time-course transcription reactions, while Tadigotla *et al* is unsuited for this type of kinetic prediction. More importantly, the two models in general predict different pausing mechanisms even for the same pausing sites, and the Bai *et al* model provides an explanation more consistent with recent single molecule observations.

Keywords: molecular motors (theory), molecular motors (experiment), single molecule

J. Stat. Mech. (2010) P12007

[1] Author to whom any correspondence should be addressed. Present address: The Rockefeller University, New York, NY 10065, USA.

1742-5468/10/P12007+16$30.00

Contents

1. Introduction

Transcription elongation is a process by which RNA polymerase (RNAP) copies genetic information from DNA into RNA. During elongation, RNAP translocates on a DNA template and incorporates NTPs (nucleoside triphosphates) into the $3'$ end of the nascent RNA. The rate of incorporation of each NTP is far from uniform, and is largely dictated by the DNA sequence being transcribed. In particular, at certain sequences known as pause sites, RNAP tends to dwell much longer than on average (for review see [1]). Pausing reflects the intrinsic kinetic properties of transcription elongation and, moreover, some pause sites have been found to play important regulatory functions in gene expression [2, 3]. Therefore, establishing a correlation between the DNA sequence and pausing would be an essential step in understanding both the transcription mechanism and gene regulation.

Biochemical assays have shown that at some pause sites, RNAP reverse translocates by threading the $3'$ RNA into its secondary channel, a phenomenon known as backtracking [4, 5]. Backtracking can be viewed as a non-productive branch pathway that kinetically competes with the main pathway of NTP incorporation [1, 6]. With improved spatial resolution to near bp level, recent single molecule experiments revealed

doi:10.1088/1742-5468/2010/12/P12007

that although pauses of longer duration could be induced by backtracking, pauses of shorter duration showed no or minimal backtracking [7, 8] and thus are likely caused by a different mechanism.

Based on a thermodynamic analysis of the transcription elongation complex (TEC) pioneered by Yager and von Hippel [9], a kinetic model developed by Bai *et al* [10, 11] (referred to here as Model B) and later a related equilibrium model by Tadigotla *et al* [12] (referred to here as Model T) now make it possible to predict pause locations and mechanisms for a given DNA sequence. These theoretical studies have provided important insights by predicting pause locations based on the free energy of the corresponding TEC, which depends strongly on the DNA sequence [9]–[13]. Although the two models have similar energetic considerations, they treat the backtracking kinetics differently: in Model B, backtracking at most template positions is considered to be a slow process and therefore insignificant compared with NTP incorporation along the main pathway; while in Model T, RNAP was allowed to undergo fast backtracking until it encountered the first secondary structure formed in the nascent RNA. These are fundamental differences and consequently are expected to generate different predictions on pause locations, kinetics, and mechanism.

Since these two models serve as valuable tools to predict sequence-dependent pausing for future elongation kinetic studies, the transcription field will benefit from a careful evaluation of these two models against relevant experimental data. Although the two models were compared by Tadigotla *et al* [12], the comparison was carried out with incorrect criteria for Model B and also only focused on predictions of pause locations at low NTP concentrations. Furthermore, the predictive power of Model B has since been improved by incorporating NTP-specific kinetic parameters [11].

In this work, we present a comprehensive comparison of Model B with Model T. (a) In an effort to make a direct and fair comparison of the two models, we reproduced Model T and checked that it predicted essentially identical pause locations to those by Tadigotla *et al* [12]. (b) We compared the predictive power of the two models by analyzing pause locations at different NTP concentrations. (c) We simulated transcription gels with Model B and Model T and evaluated their kinetic predictions against corresponding experimental transcription gels. (d) Finally we tested whether these models would provide explanations consistent with recent single molecule measurements of sequence-resolved pausing.

2. Results

Below we have briefly recapitulated Model T and Model B, described our reproduction of Model T, and then compared performance of the two models against various experimental data. Detailed experimental and simulation conditions, model parameters, and temperature considerations can be found in section 10.

3. Brief recapitulation of the two models

Both models are based on a thermal ratchet mechanism for transcription elongation: RNAP translocates reversibly between different states under thermal activation, and NTP incorporation biases RNAP to move forward by 1 bp along the DNA template. Right after NTP incorporation, the TEC is in its pre-translocation state, and the RNAP needs to translocate 1 bp downstream into the post-translocation state in order to incorporate the next NTP (first row in figure 1(A)). As mentioned above, TEC can also potentially

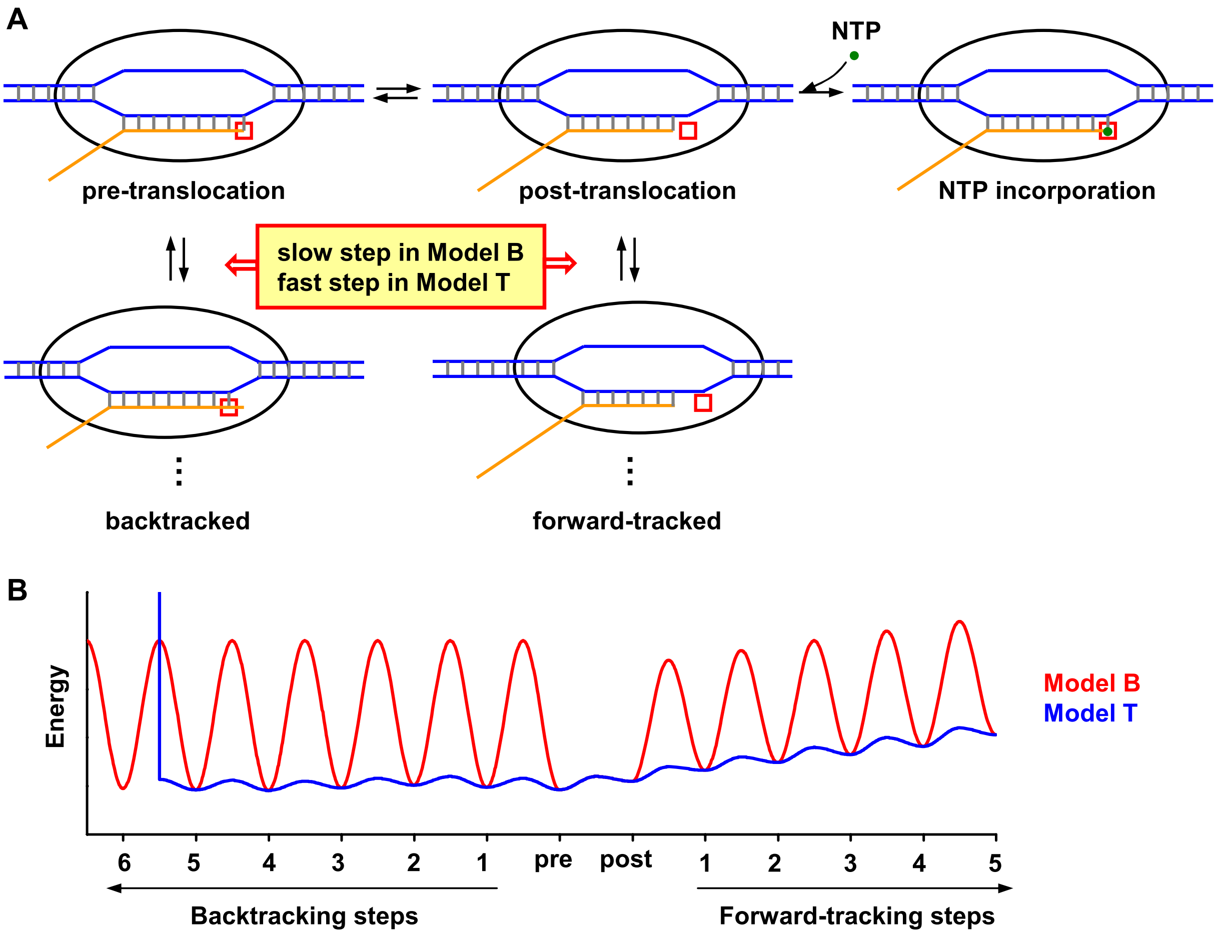

Figure 1. Overview of the two models. (A) Cartoon of the transcription elongation pathway. During elongation, the RNA polymerase unwinds a stretch of dsDNA (blue), with one strand forming a double helix with the nascent RNA (orange). The transcription elongation complex (TEC) has different translocation states, which are defined by the relative locations between the RNA 3′ end and the RNAP active site (red box): in the pre-translocation state, the RNA 3′ end is inside the active site; in the post-translocation state, the active site is empty and the RNA 3′ end is in its immediate vicinity. Only in this position is the TEC able to bind and incorporate the incoming NTP (green dot); in the backtracked state, the RNA 3′ end passes the active site into the secondary channel; in the forward-tracked state, the RNA active site moves further downstream from the RNA 3′ end, resulting in a shortened DNA–RNA hybrid. The pathways used in the two models are almost identical, and as indicated in the plot, the main difference lies in the kinetic rates in the branch pathways (see text for details). (B) Typical translocation energy landscapes in Model B (red) and Model T (blue). The troughs of the curves represent the TEC free energy in different translocation states, and the peaks in between neighboring troughs are the activation barriers that affect the translocation rate. In general, the energy barriers for backtracking and forward-tracking in Model B are much higher than those in Model T.

access the 'backtracked' or 'forward-tracked' states (second row in figure 1(A)). During backtracking, RNAP translocates along the upstream DNA template while threading the $3'$ end of the nascent RNA through its secondary channel. During forward-tracking, RNAP moves forward beyond the post-translocation state without NTP incorporation while shortening the DNA:RNA hybrid.

Because NTP incorporation can only take place in the post-translocation state, all the other states accessible to RNAP are effectively competitive inhibitors to the elongation reaction [6]. The overall NTP incorporation rate is thus largely determined by the probability of RNAP being in the post-translocation state, which depends on the translocation energy landscape (typical examples are shown in figure 1(B)). The troughs in figure 1(B) represent the free energy of TEC in different translocation states, and the peaks in between the neighboring troughs are the activation barriers for translocation. The two models incorporated essentially the same TEC free energy (section 10), whereas they have different assumptions about the activation barriers (figure 1(B)).

The TEC free energy is calculated based on the free energy involved in ssDNA bubble and RNA–DNA hybrid formation, and its value strongly depends on the DNA sequence within the TEC, the TEC structure, and its translocation state [9, 10, 12]. TEC containing shorter RNA–DNA hybrid tends to be less stable. Therefore, the forward-tracked (hybrid length <8) and post-translocation states (hybrid length: 8) on average are less stable than pre-translocation and backtracked states (hybrid length: 9). Such an energy profile makes a simple equilibrium assumption problematic. If the TEC were to equilibrate among all translocation states, a significant portion of the RNAP would necessarily undergo extensive backtracking at a majority of the template positions, which would prevent efficient NTP incorporation during active elongation.

To reduce the probability of backtracking, the two models took different approaches. Model B assumes a large backtracking activation barrier for all the backtracking steps so that at a majority of the template positions, backtracking occurs with a low probability (red curve in figure 1(B); [10]). Model T assumes RNAP is capable of fast backtracking until it encounters the first secondary structure formed by the nascent RNA outside the RNAP, where the backtracking barrier is effectively infinite (blue curve in figure 1(B); in this particular case, RNAP encounters RNA secondary structure after 5 bp backtracking). In other words, the most significant difference between the two models is the accessibility of RNAP to its backtracked states. Model B also assumes a higher forward-tracking barrier (figure 1(B)), but since the forward-tracked states are unstable, the forward-tracking rates do not significantly affect the model prediction.

Model T consists of five alternative sub-models [12]: four equilibrium models with and without the consideration of co-transcriptional RNA folding and thermal fluctuation of the TEC structure, and one kinetic model. These models are highly related, and are supposed to illustrate the contributions made by the various energetic components to the predictive power, within the same conceptual equilibrium model. The consideration of the folded RNA is a unique and important component of Model T but the fluctuations in the TEC structure have only a small quantitative effect on the model performance [12]. Also, Model T's kinetic sub-model produced predictions similar to its equilibrium counterpart. Therefore, in this work, we focus on the comparison of Model B with Model T's 'SBF' sub-model (single bubble with RNA folding, i.e., the equilibrium model with RNA folding and single TEC structure).

4. Replication of Model T

In order to make direct and valid comparisons of the two models, we reproduced Model T (the SBF sub-model) and checked for pause locations on the same ten sequences as were used by Tadigotla *et al* [12] (section 10).

In Model T, because of the equilibrium assumption, the NTP incorporation at any site, n, follows single exponential kinetics with a rate constant $k(n)$. A pause is defined when the $k(n)$ falls below a threshold: $k(n) < \xi \max\{k(n)\}$, where $\max\{k(n)\}$ is the maximum $k(n)$ on that template at a given NTP concentration. We tuned ξ to achieve maximum predictive power of pause locations, defined as the ratio of correct to incorrect pause location predictions. The optimized ξ is equal to 0.015, identical to that used in the original Model T, resulting in ∼30% of the sequence being pause sites. The pause sites predicted by our implementation of Model T had ∼95% overlap with those predicted by the original Model T (see the Supplementary Information, hereafter referred to as SI), and the overall predictive powers of the two versions were essentially identical (figure 2(A)). Note that in figure 2, we plotted the inverse of the predictive power, i.e., the ratio of incorrect to correct pause location predictions. This presentation follows the notation of Tadigotla *et al* [12] in order to make a straightforward comparison with their figure 2B.

This good agreement indicates that we have faithfully reproduced Model T. The minor differences in their pause predictions may be due to details of pause selection (section 10). In the following sections, we will only compare Model B with our implementation of Model T.

5. The two models have similar predictive power at low [NTP]

Previously, Tadigotla *et al* [12] compared the two models for their predictions of the pause locations on ten templates, where the pauses were identified experimentally at low NTP concentrations ($\leq$40 μM NTPs), and concluded that Model T had much better predictive power than Model B. However, the predictive power of pause locations in both models depends strongly on the pause criteria, which were optimized for Model T, but not for Model B. In addition, Model B recently incorporated NTP-specific kinetic parameters [11], which improved its accuracy in kinetic predictions. Therefore, we repeated the comparisons of Model T with Model B (2004) and Model B (2007) with pause criteria individually optimized for each model.

The pause criteria used in Model T cannot be directly applied to Model B because in Model B backtracked states are not in equilibrium with pre- and post-translocation states, and thus NTP incorporation cannot be simply characterized by a single rate constant. Instead, we set a threshold for the average RNAP dwell time at each template position, $\tau(n)$. By analogy with Tadigotla *et al* [12], a pause is defined when $\tau(n) > (1/\eta) \min\{\tau(n)\}$, where $\min\{\tau(n)\}$ is the shortest $\tau(n)$ on the template at a given NTP concentration. We tuned η for Model B to achieve maximum predictive power of pause locations for the same 10 DNA sequences as were used for Model T. The optimized $\eta \sim 0.05$ resulted in ∼19% sequence coverage of pause sites.

With the optimized pause criteria, the two models generated largely overlapping predictions of pause sites (SI) and the overall predictive powers were very similar with only a slightly lower performance by Model B (2004) (figure 2(A)). This result contradicts

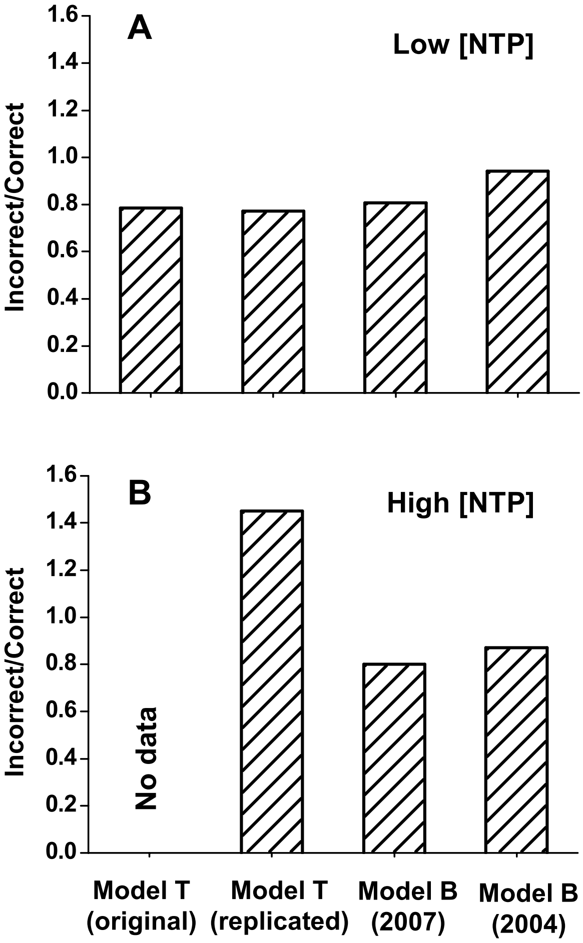

Figure 2. Comparison of the predictive powers of pause locations of the two models. The statistics of the model predictions of pause locations are illustrated by the ratio of the number of incorrect to the number of correct predictions for all templates tested. The lower the ratio is, the better the model performance. (A) Comparison at low [NTP] using the ten templates of Tadigotla *et al* [12]. (B) Comparison at high [NTP] using pKA2, pTS147 [10], $\lambda tR1$ [10], and *his* and *ops* templates [8]. First column: reported by Tadigotla *et al* [12] (see their figure 2D, only available for low [NTP]). Second column: by replicated Model T. Third column: by Model B (2007). Fourth column: by Model B (2004).

the results shown in figure 2D of Tadigotla *et al* [12], leading to the statement regarding 'the poor performance of the model presented by Bai *et al*' compared with Model T. In fact these similar results between the two models under low [NTP] reflect the overlap in the formulation of the two models: pause sites occur at unstable post-translocation states.

The pause criteria above could also be expressed as a threshold in the pause duration. The pause threshold for Model T is ∼0.15–0.30 s using $k_{\max} = 700\ \mathrm{s}^{-1}$ and $K_\mathrm{d} = 20\ \mu\mathrm{M}$ (same values as used by Tadigotla *et al* [12]), whereas it is ∼1.5–3.0 s for Model B. As discussed below, a pause threshold of the order of a second is more consistent with experimentally measured pause kinetics.

6. Model B has better predictive power at high [NTP]

Although the two models have similar performance for predictions of pause locations at low [NTP], it is possible for their performance to be different at higher [NTP]. Model T has a more stringent equilibrium assumption: Model T requires that all translocation states must reach equilibrium, whereas Model B only requires that pre- and post-translocations be in equilibrium. The equilibrium assumption is less likely to be valid when the NTP incorporation cycle is fast at high [NTP] as has been pointed out by Tadigotla *et al* [12]. It would be interesting to examine how Model T and Model B perform at high [NTP].

We compared the predictive power of pause locations by both models with measurements at higher [NTP] (100 μM–1 mM NTPs). These measurements included pauses identified on transcription gels of three templates derived from pKA2, pTS146 and λtR1 (transcription gels shown in [10]), as well as single molecule measurements on the *his* and *ops* templates [8]. As for low [NTP], pause thresholds were individually optimized for Models T and B (SI). Model B showed similar predictive power at high [NTP] to that at low [NTP], whereas the predictive power of Model T was significantly lower at high [NTP] and was about half that of Model B (figure 2(B)).

This indicates that at high [NTP], although post-translocation states may be considered in equilibrium in Model B, equilibrium among all translocation states, which is necessary for Model T, cannot be achieved. As [NTP] increases, the equilibrium assumption in Model T begins to become less valid at some template positions. The point of transition for each template position depends on sequence-dependent TEC stability and NTP-specific kinetic parameters [11], [14]–[16]. Figure 2 also shows that Model B (2007) performs better than Model B (2004) at both high and low [NTP].

7. Pause kinetics predicted by Model B, but not Model T, agrees with experiments

Pause location prediction provides a simple method to compare the two models; however, a more stringent comparison is the ability to predict pause kinetics. Conventionally pause kinetics has been assayed by time-course reactions using transcription gels. Previously we had simulated transcription gels using Model B [10] and shown that elongation and pause kinetics predicted by Model B were in good agreement with experimental transcription gels. Here using Model B [11], we simulated some of the transcription gels used in Tadigotla *et al* [12], and two examples are shown in figure 3 together with the corresponding experimental gels (D387 (A) and D167 (B) templates) [16]. The simulated gels captured most features of the experimental gels, such as the pause positions and their intensity changes over time.

These simulations also provide verification for the pause thresholds used in Model B. Note that the simulated gels had a time point interval of 15 s, but a pause does not have to be >15 s in duration to be detectable. In fact, the majority of the predicted pauses indicated in figure 2 had durations shorter than 15 s and were typically 2–5 s (SI). Yet most of them (~91%) accumulated significant populations (>2%) in at least one gel lane, which has been shown to be easily detectable in real transcription gels (for another example, see figure 3 of [10]). Thus the ~1.5 s pause threshold used by Model B was experimentally verified, in spite of the concerns raised by Tadigotla *et al* [12] that it was too short.

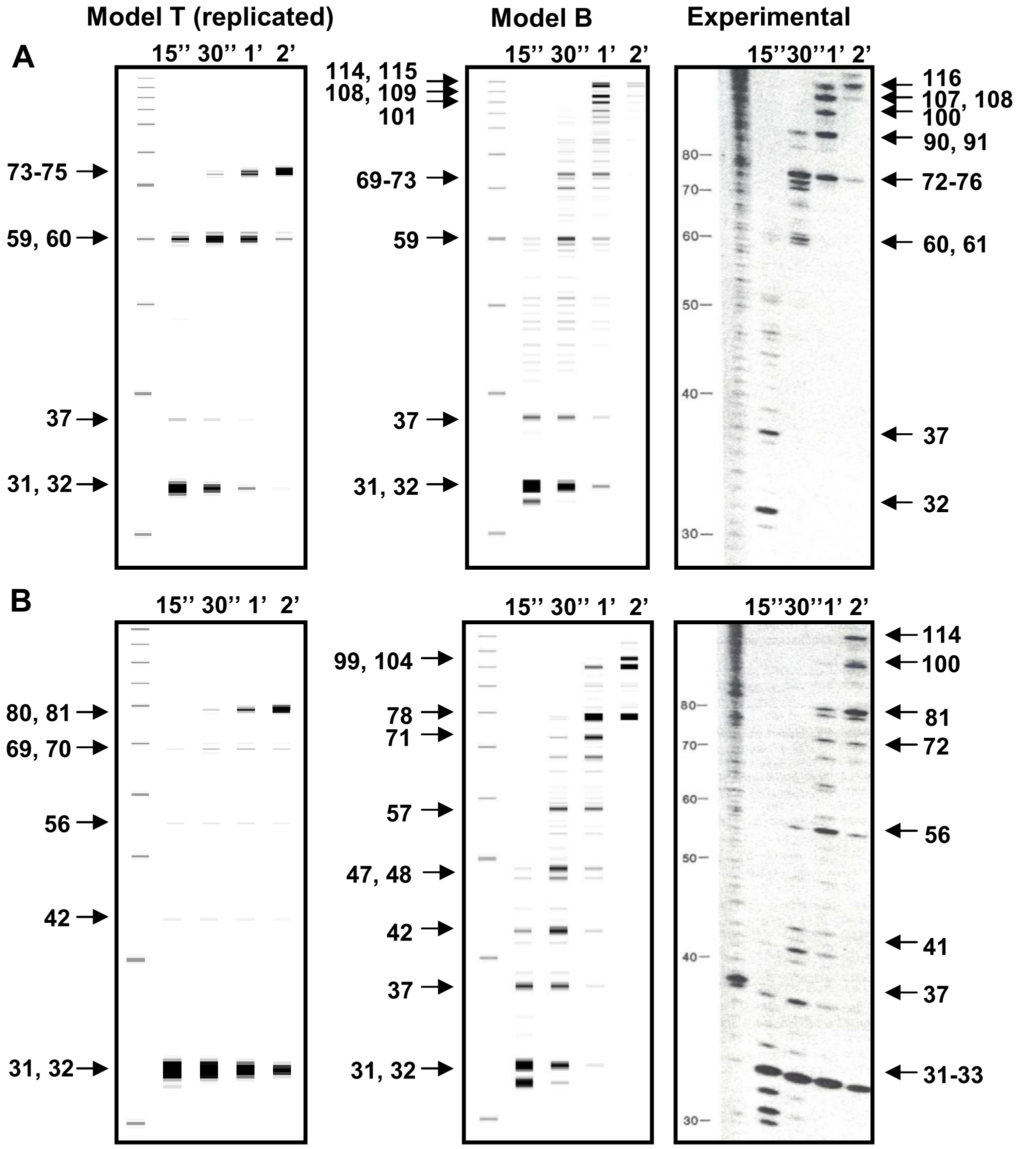

Figure 3. Prediction of transcription gels using Models T and B. (A), (B) Transcription gels on D387 (A) and D167 (B) templates [16] and the corresponding simulations using Model T and Model B (2007). Predicted prominent pauses (marked on the left side) are at similar locations with similar durations to those of measured pauses (marked on the right side).

The simulated transcription gels on the same templates using Model T could not correctly match measurements (figure 3). The predicted pause durations varied from ~0.2 s, which was too short to be detected in the corresponding gels, to ~20 min (SI), which was much longer than that estimated from the gel (<1 min). It is important to note that the pause kinetics predicted by Model T cannot be corrected by a simple linear rescaling of rates at all sites (e.g., using a different $k_{\max}$), which does not change the dynamic range of $k(n)$ (over six orders of magnitude). Nevertheless, it is likely that this dynamic range may decrease if the alternative 'MBF' (multiple bubbles with RNA folding) and kinetic sub-models are used.

8. The two models predict different pause mechanisms

Because the two models have different treatments of translocation into backtracked states, they predict different translocation states that RNAP may explore prior to the next NTP incorporation. For a given template position n, the translocation states of RNAP may be characterized by the mean translocation state $\bar{m}|_n$ ($m < 0$ for backtracked states, $m = 0/1$ for pre- and post-translocation states, and $m > 1$ for forward-tracked states; section 10).

Tadigotla *et al* [12] assumed that RNAP may rapidly backtrack until it encounters a secondary structure in RNA. Because backtracked states in general are more stable than the post-translocation state, Model T predicts significant backtracking of RNAP, especially at pause sites. Over the ten templates used by Tadigotla *et al* [12], Model T predicts that $\bar{m}|_n = -1.6 \pm 3.3$ bp (mean ± sd) for all the template positions including pause and non-pause sites, and -4.2 ± 4.0 bp for pause sites alone (figure 4(A)).

On the other hand, Model B predicted two different types of pauses [10], one involves backtracking and the other is caused by repetitive translocation between pre- and post-translocation states. Due to the high backtracking activation barrier in Model B, backtracking occurs with small probability. For instance, out of the 91 pauses predicted by Model B on the ten templates, only 15 had a backtracking probability >5%. Accordingly, this low probability of backtracking results in $\bar{m}|_n$ being close to the pre-translocation state. Over the ten templates, Model B predicts that RNAP is always located close to the pre-translocation state: $\bar{m}|_n = 0.3 \pm 0.3$ bp for all template positions, and 0.0 ± 0.19 bp for pause sites (figure 4(A)).

We compared predictions by the two models with single molecule measurements by Herbert *et al* [8], where the $\bar{m}|_n$ at certain pause sites were directly measured with near bp resolution. In total, six pause sites were examined and no significant RNAP backtracking was found at these pauses (figure 4(B); [8]). Incorporating the 7 pN assisting force applied to the RNAP by tilting the energy landscape [11, 17], both models were able to predict four out of the six pause sites (figure 4(B)). However, the $\bar{m}|_n$ predicted from the two models are different: over the four pause sites, Model T predicted that RNAP can backtrack by as much as ∼7 bp. This large backtracking distance resulted in a difference between the predicted and measured paused position of RNAP by as much as ∼9 bp, much larger than the measurement uncertainty. In contrast, in agreement with the measurements, Model B predicted that $\bar{m}|_n$ values at the pause sites are all close to 0 (no significant backtracking) (figure 4(B)).

We have also compared the predicted apparent step size ($\bar{m}|_{n+1} - \bar{m}|_n + 1$) distributions of RNAP during transcription elongation from the two models with single molecule measurements conducted at 18 pN assisting force [7]. Both models have an intrinsic mean apparent step size of 1 bp; however they predict markedly different distributions (figure 4(C)). On the template used by Shaevitz *et al*, Model T predicted an apparent step size variation of 1.0 bp (sd). This large variation is inconsistent with the experimental observation that RNAP took uniform 1 bp steps with variations ∼0.2 bp. Model B, on the other hand, predicted an apparent step size variation of 0.4 bp, again more in accord with measurements.

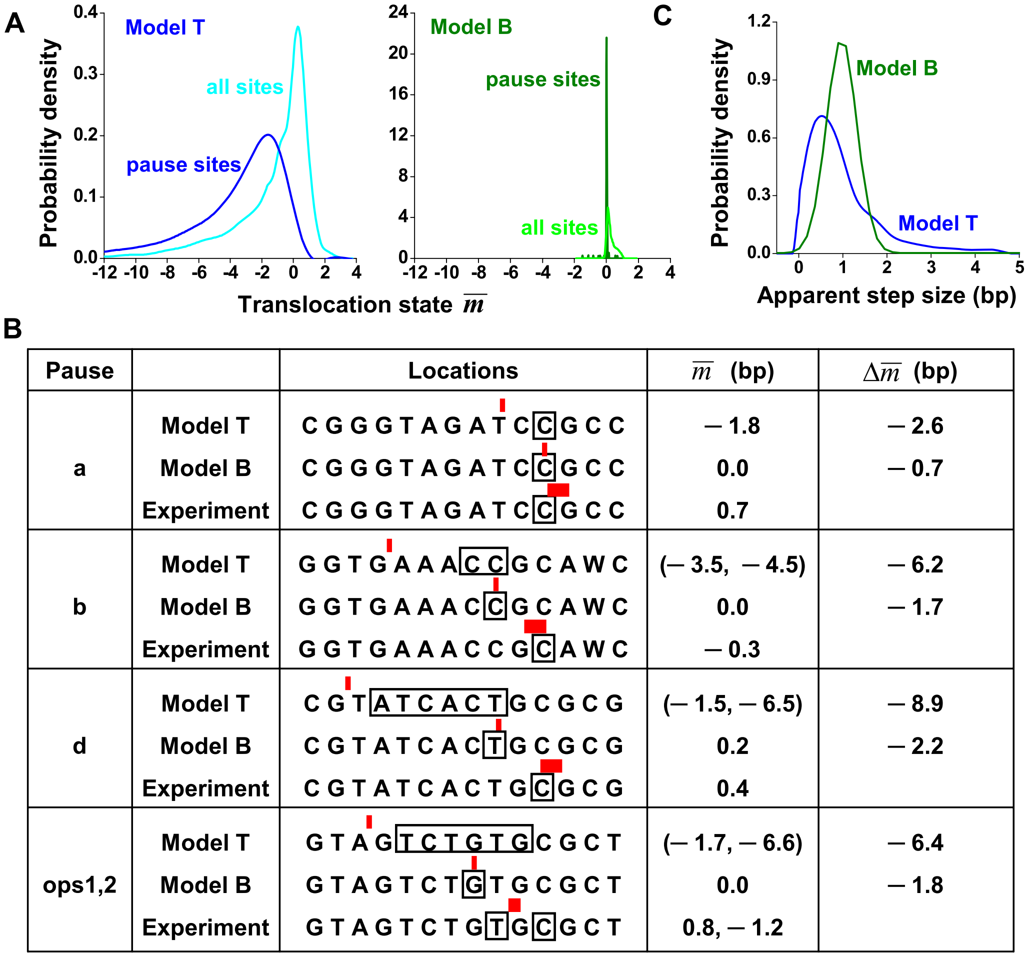

Pause		Locations	$\overline{m}$ (bp)	$\Delta\overline{m}$ (bp)
a	Model T	CGGGTAGATC$\boxed{C}$GCC	− 1.8	− 2.6
	Model B	CGGGTAGATC$\boxed{C}$GCC	0.0	− 0.7
	Experiment	CGGGTAGATC$\boxed{C}$GCC	0.7	
b	Model T	GGTGAAA$\boxed{CC}$GCAWC	(− 3.5, − 4.5)	− 6.2
	Model B	GGTGAAAC$\boxed{C}$GCAWC	0.0	− 1.7
	Experiment	GGTGAAACCG$\boxed{C}$AWC	− 0.3	
d	Model T	CGT$\boxed{ATCACT}$GCGCG	(− 1.5, − 6.5)	− 8.9
	Model B	CGTATCAC$\boxed{T}$GCGCG	0.2	− 2.2
	Experiment	CGTATCACTG$\boxed{C}$GCG	0.4	
ops1,2	Model T	GTAG$\boxed{TCTGTG}$CGCT	(− 1.7, − 6.6)	− 6.4
	Model B	GTAGTCT$\boxed{G}$TGCGCT	0.0	− 1.8
	Experiment	GTAGTCTG$\boxed{T}$G$\boxed{C}$GCT	0.8, − 1.2	

Figure 4. Comparison of the prediction of pause mechanism. (A) The predicted histogram of the mean translocation state $\bar{m}|_n$ by Model T (left) and Model B (2007) (right) for all positions, or for pause sites alone, on the ten templates used in Tadigotla *et al* [12]. (B) Comparison of the predicted and measured [8] translocation states of the pause sites from the *his* and *ops* templates. For the experimental data, each red bar indicates pause position measured by single molecule techniques and the width of the bar indicates the uncertainty in the measurement; each black box indicates the location of the 3′ end of the RNA during pausing as determined by a transcription gel. The distance between the bar and the box thus indicates the RNAP translocation state at the pause site. Similar notation is used for predictions by the two models. Model B predicted a single pause site with a single RNAP position on the DNA template for each sequence. On the other hand, Model T predicted multiple pause sites for some sequences but a single location of RNAP on the DNA template during pausing. The two columns on the right show the distance of the RNAP on the DNA template from the pre-translocation state, and the difference in the predicted and measured position of RNAP. (C) RNAP apparent step size distributions predicted by Model T and Model B under 18 pN assisting force.

9. Discussion

In this work, we have compared two recent models on sequence-dependent kinetics of transcription elongation. We conclude that Model B has an overall better performance than Model T in terms of predictive power of pause location, kinetics, and mechanism. Nonetheless, a major strength of Model T is its simplicity compared with Model B. It involves fewer model parameters that must be experimentally determined.

The two models share a large degree of similarity in their formulations. Their major differences lie in their different RNAP backtracking kinetics and how to consider the effect of co-transcriptional RNA folding on the elongation kinetics. Below we will elaborate on these two points and discuss the pros and cons for each model.

In Model B, the backtracking 'entry step' (from the pre-translocation state to the first backtracked state) is in general assumed to be slow compared to the NTP incorporation rate in the main reaction pathway so that backtracking happens with very low probability for most template positions. As a result, a majority of predicted pauses are pre-translocation pauses that occur along the main reaction pathway. In Model T, backtracking is assumed to be very rapid until RNAP encounters a kinetic barrier imposed by co-transcriptionally folded RNA. Thus most of the predicted pauses by this model are backtracked pauses.

Biochemical experiments indicate slow translocation kinetics into and out of a backtracked state: on some experimentally identified backtracked pause sites, RNAP only backtracked under prolonged NTP starvation of $\sim$10 min, which is orders of magnitude longer than the NTP incorporation timescale (0.05–1 s) [4]. In addition, single molecule experiments also indicate that most of the pauses are not caused by backtracking [7, 18]. Taken together this indicates it is likely that backtracking indeed encounters a high activation barrier as is assumed in Model B. This high barrier may be imposed by the RNAP structure that requires the $3'$ end of the nascent RNA chain to reverse thread through a narrow pore of the secondary channel (12–15 Å wide) that is tailored for NTP entry to the active site [19, 20]. Nonetheless Model B's assumptions that the barrier heights were sequence-independent and remained the same for all backtracked states are likely oversimplified. The nature of the activation barrier requires further elucidation.

The effect of co-transcriptional RNA folding on the elongation kinetics is considered in Model T, but is ignored in Model B. Secondary structures in the nascent RNA are known to play important roles in transcription kinetics. A strong RNA hairpin with a GC-rich stem, together with an adjacent downstream U-rich region, leads to termination. RNA hairpins may also induce pausing by interacting with the flap region of the RNAP [5, 21]. Therefore, a more accurate description of sequence-dependent RNAP kinetics should consider contributions from RNA secondary structures. This consideration also provides a good starting point for future modeling of transcription termination.

As pointed out in Tadigotla *et al* [12], the energetic consideration of the interplay between the backtracked RNAP and RNA secondary structure in Model T is oversimplified. More accurate modeling of RNA requires detailed knowledge of the kinetics of RNAP translocation and co-transcriptional RNA folding, which needs future effort in both experimental and theoretical work.

Although Model B has an overall better performance, RNAP kinetics might be best described by the essence of the two models: RNAP backtracks with a relatively slow rate so that at most of the template positions, backtracking occurs with low probability. Backtracked RNAP could be assisted by RNA folding to bias its motion in the forward direction. A more comprehensive description of transcription may even involve consideration of the interaction between the RNAP and downstream DNA [22], as well as RNAP conformational changes.

To test the extent of the RNA folding contribution to elongation kinetics, several experiments could be conducted. Potential pause sequences may be engineered into templates with and without strong upstream hairpins to examine the differences in pausing kinetics. RNA hairpin formation could also be eliminated to test whether backtracking is encouraged as a result. One recent single molecule study measured elongation kinetics by applying a large force on the nascent RNA to prevent formation of RNA secondary structures, and concluded that an RNA hairpin had no effect on the kinetics [23]. However, a possible effect might have been masked by the large assisting force (∼30 pN) applied to RNAP, which was previously shown to reduce backtracking [24, 25]. Alternatively, RNA hairpins could be eliminated by degrading RNA with RNase, and the RNAP elongation rate measured in a single molecule assay.

There are alternative interpretations of the pause mechanism. Herbert *et al* [8] proposed an off-pathway 'pause state' that does not involve backtracking. Biochemical studies also provided evidence that the RNA 3′-end in TEC could 'fray' from the template DNA and thus induce pausing off the main reaction pathway [26, 27]. It should be noted that if the occurrence of such an isomerization step is correlated with the equilibrium of the pre/post-translocation state, it would not change the predicted pause sites from the current Model B.

Our hope in the current work is to put forth a comprehensive comparison of the current models in an effort to clarify the strengths and weaknesses of each model and to lay out a foundation for future theoretical and experimental work on the mechanism of sequence-dependent transcription pausing and elongation.

10. Materials and methods

10.1. Experimental and simulation conditions

If not mentioned specifically, the NTP concentrations used in the simulations are the same as the corresponding experiments: (1) low [NTP]: 10 μM for sequences D104, D111, D112, D123, D167, D387 (30 °C; [16]), 40 μM for sequence seq10, and 30 μM for sequences seq11–seq13 (30 °C; [12]); (2) high [NTP]: 1 mM for pKA2, 1 mM ACG, 200 μM U for pTS147, 100 μM for λtR1 (25 °C; [10]), and 1 mM ACU, 250 μM G for *his* and *ops* templates (∼25 °C; [8]); and (3) step size simulation: 5 μM A, 2.5 μM C, 10 μM G/UTP. These conditions are listed in a table in SI.

10.2. Temperature considerations

As shown above, experiments were conducted at different temperatures. Since model parameters including those relating to the thermodynamic stability of nucleic acids and kinetic rates are functions of temperature, these parameters should be chosen or tuned for the temperature of the corresponding experimental measurements. However, we found that the pause location predictions by both models were rather insensitive to model parameters, in agreement with Tadigotla *et al* [12]. On the other hand, we also found that the pause kinetics was very sensitive to temperature. Therefore, the following treatments of temperature were taken in the considerations of Model T and Model B.

In order to faithfully replicate Model T, we performed simulations of pause location data under low [NTP] for Model T using thermodynamic parameters for 37 °C, which is different from the experimental temperature of 30 °C but is the same as was used by Tadigotla *et al* [12]. We performed simulations of pause location data under high [NTP] using thermodynamic parameters for 25 °C, the same as the experimental temperature.

The parameters for Model B have previously been optimized for 25 °C [10, 11]. Here all pause location predictions were performed using the same parameters. Kinetic predictions, such as simulations of transcription gels, require more careful consideration of temperature. Since the experimental transcription gels shown in figure 2 were taken under 30 °C, to compensate for the increased transcription rate at 30 °C, we increased the [NTP] from the experimental concentration of 10–25 μM.

10.3. Parameters used in the simulation

The same structure of TEC was used for both models: a DNA bubble size of 12 bp, a DNA–RNA hybrid size of 9 bp, and 1 nt downstream ssDNA. For Model T, the $k_{\max}$ and K_{d} were the same as in Tadigotla *et al*: $k_{\max}$: 700 s^{-1}, K_{d}: 20 μM. For Model B, the NTP-dependent $k_{\max}$ and K_{d} were the same as in [11], the backtracking barrier height was 41.2 $k_{\mathrm{B}}T$, and the rest of the parameters were the same as in [10].

10.4. Subtle differences in the model consideration

In Model B, we consider a dangling energy term for the post-translocation and forward-tracked state energies by assuming a 50% terminal base pair energy for the ss template DNA nucleotide immediately adjacent to the 3$'$ end of the RNA in the transcription bubble [9, 10]. This term is not considered by Tadigotla *et al* and their replicated model.

In Tadigotla *et al*, the TEC state energy includes the RNA folding energy. For a given product length n, RNA folding is only considered for pre- and backtracked states and a folded RNA structure does not unfold until after NTP incorporation. Therefore, RNAP will not move beyond the first hairpin encountered. In a sense, this is not an equilibrium model. Strictly speaking, were RNA also allowed to fold in forward-tracked states, RNAP would often become arrested or dissociated because of the lack of RNA unfolding assumed in the model. Even if the unfolding rate were assumed to be fast, the forward-tracked states would then be in equilibrium with all the other accessible states; there would be cases where RNAP would pause because forward-tracked states are energetically more favorable. These pauses were manually discarded by Tadigotla *et al* because of the argument that RNAP's transient presence in the forward states did not allow enough time for hairpin formation (personal communication). In order to faithfully reproduce Model T, we also did not allow hairpins to form in forward-tracked states so that the RNA folding energy stayed the same for the forward-tracked states as that of the post-translocation state. Because energetically favorable forward-tracked states are very rare, this treatment in the energy calculation in Model T does not significantly affect its predictions.

10.5. Calculation of $\bar{m}|_n$

In Model T, the average translocation position at site n relative to the pre-translocation state was calculated as

$$\bar{m}|_n = \frac{(1 + ([\mathrm{NTP}]/K_\mathrm{d}))\exp(-\Delta G_{n,1}/k_\mathrm{B}T) + \sum_{m\neq 1} m \exp(-\Delta G_{n,m}/k_\mathrm{B}T)}{(1 + ([\mathrm{NTP}]/K_\mathrm{d}))\exp(-\Delta G_{n,1}/k_\mathrm{B}T) + \sum_{m\neq 1} \exp(-\Delta G_{n,m}/k_\mathrm{B}T)}.$$

In Model B, we used a Monte Carlo method to simulate a large number of single molecule traces of RNAP position versus time. Then, for a particular n, we analyzed the total time RNAP spent at each m, $t(n,m)$, and calculated the $\bar{m}|_n$ as $\bar{m}|_n = (\sum_m m \cdot t(n,m)/\sum_m t(n,m))$.

Acknowledgments

We thank members of the Wang lab and P von Hippel for commenting on the manuscript, and V R Tadigotla, and A E Ruckenstein for helpful advice in replicating Model T and critical reading of the manuscript. This work is supported by grants to MDW from NSF grant (DMR-0517349), NIH grant (R01 GM059849), and the Keck Foundation's Distinguished Young Scholar Award.

References

[1] von Hippel P H, *An integrated model of the transcription complex in elongation, termination, and editing*, 1998 *Science* **281** 660

[2] Roberts J W *et al*, *Antitermination by bacteriophage lambda Q protein*, 1998 *Cold Spring Harb. Symp. Quant. Biol.* **63** 319

[3] Artsimovitch I and Landick R, *The transcriptional regulator RfaH stimulates RNA chain synthesis after recruitment to elongation complexes by the exposed nontemplate DNA strand*, 2002 *Cell* **109** 193

[4] Komissarova N and Kashlev M, *RNA polymerase switches between inactivated and activated states by translocating back and forth along the DNA and the RNA*, 1997 *J. Biol. Chem.* **272** 15329

[5] Artsimovitch I and Landick R, *Pausing by bacterial RNA polymerase is mediated by mechanistically distinct classes of signals*, 2000 *Proc. Nat. Acad. Sci.* **97** 7090

[6] Guajardo R and Sousa R, *A model for the mechanism of polymerase translocation*, 1997 *J. Mol. Biol.* **265** 8

[7] Shaevitz J W, Abbondanzieri E A, Landick R and Block S M, *Backtracking by single RNA polymerase molecules observed at near-base-pair resolution*, 2003 *Nature* **426** 684

[8] Herbert K M *et al*, *Sequence-resolved detection of pausing by single RNA polymerase molecules*, 2006 *Cell* **125** 1083

[9] Yager T D and von Hippel P H, *A thermodynamic analysis of RNA transcript elongation and termination in Escherichia coli*, 1991 *Biochem.* **30** 1097

[10] Bai L, Shundrovsky A and Wang M D, *Sequence-dependent kinetic model for transcription elongation by RNA polymerase*, 2004 *J. Mol. Biol.* **344** 335

[11] Bai L, Fulbright R M and Wang M D, *Mechanochemical kinetics of transcription elongation*, 2007 *Phys. Rev. Lett.* **98** 068103

[12] Tadigotla V R *et al*, *Thermodynamic and kinetic modeling of transcriptional pausing*, 2006 *Proc. Nat. Acad. Sci.* **103** 4439

[13] Wilson K S and von Hippel P H, *Transcription termination at intrinsic terminators: the role of the RNA hairpin*, 1995 *Proc. Nat. Acad. Sci.* **92** 8793

[14] Rhodes G and Chamberlin M J, *Ribonucleic acid chain elongation by Escherichia coli ribonucleic acid polymerase. I. Isolation of ternary complexes and the kinetics of elongation*, 1974 *J. Biol. Chem.* **249** 6675

[15] Foster J E, Holmes S F and Erie D A, *Allosteric binding of nucleoside triphosphates to RNA polymerase regulates transcription elongation*, 2001 *Cell* **106** 243

[16] Levin J R and Chamberlin M J, *Mapping and characterization of transcriptional pause sites in the early genetic region of bacteriophage T7*, 1987 *J. Mol. Biol.* **196** 61

[17] Wang M D *et al*, *Force and velocity measured for single molecules of RNA polymerase*, 1998 *Science* **282** 902

[18] Neuman K C, Abbondanzieri E A, Landick R, Gelles J and Block S M, *Ubiquitous transcriptional pausing is independent of RNA polymerase backtracking*, 2003 *Cell* **115** 437

[19] Korzheva N *et al*, *A structural model of transcription elongation*, 2000 *Science* **289** 619

[20] Zhang G *et al*, *Crystal structure of Thermus aquaticus core RNA polymerase at 3.3 A resolution*, 1999 *Cell* **98** 811

[21] Toulokhonov I and Landick R, *The flap domain is required for pause RNA hairpin inhibition of catalysis by RNA polymerase and can modulate intrinsic termination*, 2003 *Mol. Cell.* **12** 1125

[22] Ederth J, Artsimovitch I, Isaksson L A and Landick R, *The downstream DNA jaw of bacterial RNA polymerase facilitates both transcriptional initiation and pausing*, 2002 *J. Biol. Chem.* **277** 37456

[23] Dalal R V *et al*, *Pulling on the nascent RNA during transcription does not alter kinetics of elongation or ubiquitous pausing*, 2006 *Mol. Cell.* **23** 231

[24] Shundrovsky A, Santangelo T J, Roberts J W and Wang M D, *A single-molecule technique to study sequence-dependent transcription pausing*, 2004 *Biophys. J.* **87** 3945

[25] Abbondanzieri E A, Greenleaf W J, Shaevitz J W, Landick R and Block S M, *Direct observation of base-pair stepping by RNA polymerase*, 2005 *Nature* **438** 460

[26] Mukherjee S, Brieba L G and Sousa R, *Discontinuous movement and conformational change during pausing and termination by T7 RNA polymerase*, 2003 *EMBO J.* **22** 6483

[27] Toulokhonov I, Zhang J, Palangat M and Landick R, *A central role of the RNA polymerase trigger loop in active-site rearrangement during transcriptional pausing*, 2007 *Mol. Cell.* **27** 406